Proc. Natl. Acad. Sci. USA
Vol. 94, pp. 9165–9170, August 1997
Developmental Biology

CENP-E is an essential kinetochore motor in maturing oocytes and is masked during Mos-dependent, cell cycle arrest at metaphase II

NICK S. DUESBERY*†, TAESAENG CHOI*†‡, KEVIN D. BROWN§¶, KENNETH W. WOOD‖, JAMES RESAU*, KENJI FUKASAWA*, DON W. CLEVELAND‖, AND GEORGE F. VANDE WOUDE*,**

*ABL-Basic Research Program, National Cancer Institute–Frederick Cancer Research and Development Center, P.O. Box B, Frederick, MD 21702-1201; §Department of Biological Chemistry, Johns Hopkins University School of Medicine, Baltimore, MD 21205; and ‖Ludwig Institute for Cancer Research and University of California at San Diego, 9500 Gilman Drive, La Jolla, CA 92093-0660

Contributed by George F. Vande Woude, June 10, 1997

ABSTRACT **CENP-E, a kinesin-like protein that is known to associate with kinetochores during all phases of mitotic chromosome movement, is shown here to be a component of meiotic kinetochores as well. CENP-E is detected at kinetochores during metaphase I in both mice and frogs, and, as in mitosis, is relocalized to the midbody during telophase. CENP-E function is essential for meiosis I because injection of an antibody to CENP-E into mouse oocytes in prophase completely prevented progression of those oocytes past metaphase I. Beyond this, CENP-E is modified or masked during the natural, Mos-dependent, cell cycle arrest that occurs at metaphase II, although it is readily detectable at the kinetochores in metaphase II oocytes derived from *mos*-deficient ($MOS^{-/-}$) mice that fail to arrest at metaphase II. This must reflect a masking of some CENP-E epitopes, not the absence of CENP-E, in meiosis II because a different polyclonal antibody raised to the tail of CENP-E detects CENP-E at kinetochores of metaphase II-arrested eggs and because CENP-E reappears in telophase of mouse oocytes activated in the absence of protein synthesis.**

In many animal species, fully grown germ cells are arrested at prophase of meiosis I as immature oocytes [germinal vesicle (GV)-stage oocytes]. Upon hormonal stimulation, oocytes resume meiosis (mature), and eventually arrest at metaphase II (MII) as unfertilized eggs. Masui and Markert (1) observed that when cytoplasm from MII-arrested eggs was transferred to one blastomere of a 2-cell embryo, the injected blastomere arrested division at metaphase. This led them to hypothesize that a cytoplasmic factor, called cytostatic factor (CSF), was responsible for MII arrest. The Mos protooncogene product has been shown to be an active component of CSF (2); it is expressed and functions during oocyte meiosis (3–8), and its injection into blastomeres causes metaphase arrest (8). In addition, oocytes of $Mos^{-/-}$ mice fail to arrest at MII and undergo parthenogenic activation (9–11). More recently, mitogen-activated protein kinase (MAPK), a downstream effector of Mos (12–14), has also been shown to induce metaphase arrest in injected blastomeres (15, 16).

Although Mos and MAPK have been implicated in the reorganization of microtubules (MTs) (17–19) and meiotic spindle formation (9, 20), our understanding of the manner in which CSF brings about MII arrest remains largely unknown. It has been proposed that the Mos/MAPK pathway functions to maintain maturation promoting factor (MPF) activity, most likely through preventing cyclin B degradation (2, 21, 22). However, when nondestructible cyclin B is present in yeast (23) or *Xenopus* extracts (24), the metaphase–anaphase transition can still be induced in the presence of high MPF activity. Thus, rather than (or in addition to) directly promoting MPF activity, the Mos/MAPK pathway may cause metaphase arrest by its action on other proteins that are essential for the metaphase–anaphase transition.

Studies of insect meiosis (25) and mitosis (26) have suggested that the mechanical balancing of kinetochore forces may play a role in metaphase arrest. The movement of chromosomes is controlled by the dynamic polymerization and depolymerization of spindle MTs as well as by MT-associated motor proteins (reviewed in refs. 27 and 28). The kinetochore, a specialized structure located at the centromere, is the site of chromosome attachment to the MTs and is thought to be associated with one or more MT motor proteins (reviewed in refs. 29 and 30.)

One such protein, CENP-E, is a >300-kDa protein consisting of three domains; a globular N-terminal head with homology to kinesin, an α-helical stalk, and a globular C-terminal tail (31). CENP-E, which is associated with MT motor activity *in vitro* (ref. 32; K.W.W. and D.W.C., unpublished work), has been shown to associate with kinetochores immediately following the breakdown of the nuclear envelope during mitosis (31, 33). CENP-E remains kinetochore-associated during mitotic chromosome movement, dissociating only after chromosome segregation is complete at anaphase A (34). Finally, beginning in anaphase B, when the spindle elongates, CENP-E relocalizes to the MTs present in the midbody of the mitotic spindle (34). Besides its location at the kinetochore, two findings have implicated CENP-E in mitotic chromosome movement: microinjection of CENP-E antibodies into HeLa cells during prometaphase partially delayed or prevented the onset of anaphase (33), and CENP-E antibodies strongly inhibited MT depolymerization-dependent movement of chromosomes *in vitro* (35).

Although to date no kinetochore-associated motor protein has been implicated in meiosis in any organism, it is reasonable to hypothesize that such an association exists, based upon observations of mitotic systems. To examine this hypothesis, we have used both mouse and *Xenopus* oocytes to determine whether CENP-E plays a role in meiotic chromosome move-

Abbreviations: GV, germinal vesicle; MII, metaphase II; MI, metaphase I; CSF, cytostatic factor; MAPK, mitogen-activated protein kinase; MPF, maturation promoting factor; MT, microtubule; DAPI, 4′,6-diamidino-2-phenylindole.

The publication costs of this article were defrayed in part by page charge payment. This article must therefore be hereby marked "*advertisement*" in accordance with 18 U.S.C. §1734 solely to indicate this fact.

†N.S.D. and T.C. contributed equally to this paper.

‡Present address: P.O. Box 61 Yu Song, Science Town, Taejon, 305–380 Korea.
¶Present address: Laboratory of Gene Transfer, National Human Genome Research Institute, National Institutes of Health, Bethesda, MD 20892.
**To whom reprint requests should be addressed.

ment and whether regulatory changes to CENP-E can account, at least in part, for CSF-mediated cell cycle arrest at MII.

MATERIALS AND METHODS

Mouse Oocytes and Eggs. GV-oocytes were collected from 3- to 4-week-old B6C3 F_1 mice or from Mos knockout mice ($Mos^{-/-}$) (9) 45–48 h after injection with pregnant mares' serum and cultured in modified Whitten's medium at 38.5°C (36). Ovulated oocytes were obtained from oviducts 15–18 h after human chorionic gonadotropin injection (5 units).

For microinjection, oocytes were transferred to Whitten's media with Hepes (mWM; PGC Scientific, Gaithersburg, MD) containing 7% fetal calf serum and 100 μM 3-isobutyl-1-methylxanthine, and injected with ≈10 pl (l) of IgG (1 μg/μl) in Dulbecco's PBS. Injected or uninjected oocytes were washed three times in mWM and matured *in vitro*.

For oocyte activation, ovulated oocytes obtained from oviducts at 16 h after human chorionic gonadotropin injection were cultured with 10 μg/ml puromycin and fixed after 2 h (anaphase/telophase) or 4 h (second polar body extrusion).

Frog Oocytes and Eggs. Mature *Xenopus laevis* were obtained from Xenopus I (Ann Arbor, MI). Collagenase or manually defolliculated oocytes were isolated and induced to mature with progesterone according to the methods of Duesbery and Masui (37). Eggs were squeezed from pregnant mares' serum-primed frogs that had been induced to ovulate by the injection of 600 units of human chorionic gonadotropin 15 h earlier and dejellied with one volume of 3% cysteine-HCl/1% NaOH. Eggs were fertilized *in vitro* according to the methods of Moses and Masui (38). When required, eggs were electrically activated.

Immunoblotting. Logarithmically growing cultures of HeLa (human) cells and L (mouse) cells were mitotically arrested by treatment with Colcemid (0.1 μg/ml) for 18 h. The mitotic cells were selected by mitotic shake-off, pelleted by centrifugation, and washed extensively with cold (4°C) PBS. The cells were then lysed by addition of 25 mM Tris·HCl (pH 7.5), 5 mM EDTA, and 1% SDS, and placed in a boiling water bath for 5 min. The protein concentration of each sample was determined and the appropriate amount of each sample was diluted in SDS sample buffer. Ovulated mouse oocytes were obtained from oviducts and denatured in SDS sample buffer by boiling for 5 min.

Lysates of whole frog oocytes, eggs, and blastulae were made according to the methods of Shibuya *et al.* (39).

Following SDS/PAGE and electrotransfer to nitrocellulose or polyvinylidene difluoride membrane, the blots were blocked and incubated overnight at 4°C in an appropriate dilution of affinity purified CENP-E polyclonal antisera. Immunoreactive bands were visualized using ^{125}I-labeled conjugated protein-A (ICN) by autoradiography (16 h at −80°C with intensifying screens) or by horseradish peroxidase (HRP)-conjugated secondary antibodies visualized by chemiluminescence (Phototope-HRP; New England Biolabs) as indicated.

Immunostaining of Mouse L-Cells, Oocytes, and Eggs. Mouse L-cells were cultured in DMEM containing 10% fetal calf serum at 37°C in the presence of Colcemid (0.1 μg/ml) for 2 h and the mitotic cells collected by mitotic shake off and harvested by centrifugation. The cells were then swollen by incubation (10 min, room temperature) in hypotonic buffer (10 mM Tri·HCl, pH 7.4/10 mM NaCl/5 mM $MgCl_2$) and pelleted onto coverslips. The cells were fixed with cold (−20°C) methanol for 5 min, rinsed in PBS, and incubated in a polyclonal antibody raised against a bacterially expressed stalk portion of human CENP-E (pAb-HpX; ref. 34) diluted in PBS containing 5% BSA. Fluorescein isothiocyanate (FITC)-labeled goat-anti-rabbit IgG was used as a secondary antibody, and DNA was visualized by propidium iodine staining.

Mouse oocytes were denuded, fixed, and washed according to the methods of Choi *et al.* (40) and incubated for 1 h at 37°C with anti-α-tubulin antibody (YL1/2) and pAb-HpX. FITC-conjugated anti-rat antibody (1:40; Boehringer Mannheim) and rhodamine-conjugated anti-rabbit antibody (1:100; Boehringer Mannheim) were used as secondary antibodies. For immunostaining of oocytes that were injected with pAb-HpX, we started the reaction with the secondary antibody, FITC-conjugated anti-rabbit antibody. Oocytes were stained with 4′,6-diamidino-2-phenylindole (DAPI) to visualize DNA. Samples were examined by confocal laser scanning microscopy. All of these confocal images were obtained using the same operating parameters.

Immunoprecipitation. Extracts of *Xenopus* oocytes or eggs were prepared according to the methods of Lohka and Maller (41), with the substitution of 10 mM bis(2-aminophenoxy)ethane-*N*,*N*,*N*′,*N*′-tetraacetate (Molecular Probes) for EGTA in the extraction buffer. Oocyte or egg extract (50 μl) diluted with 450 μl extraction buffer containing 1% Nonidet P-40 (IPEB) was mixed with 50 μl protein A-agarose (Boehringer Mannheim) that had been washed with IPEB. Samples were incubated for 3 h at 4°C and then centrifuged at 10,000 × *g* for 30 s. Ten microliters of either affinity purified pAb-XCEtail, an antibody raised to the 556 amino acid C-terminal region of *Xenopus* CENP-E, affinity purified pAb HpX, raised against the stalk portion of human CENP-E (34), or nonspecific affinity purified rabbit IgG (anti-Stat3; New England Biolabs) was then added to the supernatant. Following overnight incubation at 4°C, 50 μl of washed protein A-agarose was added and the samples were incubated for a further 3 h at 4°C. After centrifugation at 10,000 × *g* for 30 s, the pellet was washed four times for 20 min with IPEB and then 75 μl of 1× SDS-sample buffer were added and samples were heated in boiling water for 5 min. After centrifugation at 10,000 × *g* for 30 s the supernatant was analyzed by SDS/PAGE on 4% gels.

Immunostaining of Frog Oocytes and Eggs. Collagenase-defolliculated maturing oocytes, eggs, and activated eggs were immunostained using a procedure adapted from Elinson and Rowning (42). To facilitate observations of the first meiotic division, oocytes were incubated for 12 h at 4°C. This treatment causes MTs to depolymerize and allows the GV to move to the cortex of the oocyte (37, 43). Cold-treated oocytes were rinsed once with room temperature oocyte medium (44) and incubated for 0.5 h prior to use to allow the MTs to repolymerize. Samples of 10–15 oocytes or eggs were fixed in ice-cold methanol and incubated for 2–16 h at −20°C. Following rehydration through a methanol/PBS (XPBS; 145 mM NaCl/10 mM NaH_2PO_4/10 mM Na_2HPO_4, pH 7.4) series to XPBS, samples were rinsed five times for 5 min each in XPBS. Samples were then incubated in XPBS containing 0.1% Tween-20 and anti-β-tubulin (TUB 2.1; Sigma) (1:500) plus affinity-purified pAb-HpX (1:250 or 1:500) or affinity-purified pAb-XCEtail (1:500) for 12 h at 4°C. Following five rinses in XPBS for 5 min each, samples were incubated in XPBS containing 0.1% Tween-20 and fluorescein conjugated $F(ab')_2$ fragment of goat anti-mouse IgG (1:100; Boehringer Mannheim) as well as rhodamine-conjugated goat anti-rabbit IgG (1:50 or 1:100; Boehringer Mannheim) for 2 h at room temperature. Samples were then rinsed as above and cut in half at the animal–vegetal equator. The vegetal half was discarded and XPBS was replaced with 80% glycerol and 20% XPBS containing 1 μg/ml Hoechst 33342. After a few minutes the animal half was transferred to a slide and squashed beneath a coverslip. Samples were examined by confocal laser scanning microscopy. All of the confocal images presented were obtained using the same operating parameters.

RESULTS

CENP-E Is Required for the Metaphase–Anaphase Transition in Meiosis I. To test whether CENP-E is a kinetochore-

associated during meiosis of mouse ooctyes, we first examined whether a polyclonal antibody (pAb-HpX) raised against a bacterially expressed stalk portion of human CENP-E (34) could identify mouse CENP-E. When lysates of human (HeLa) cells and mouse (L) cells were enriched in mitosis by blocking spindle assembly with Colcemid, a >300-kDa polypeptide was identified in both cell types (Fig. 1*A*, lanes 1 and 3). As reported previously for the human protein (45), this protein preferentially accumulated in the mitotically arrested cells

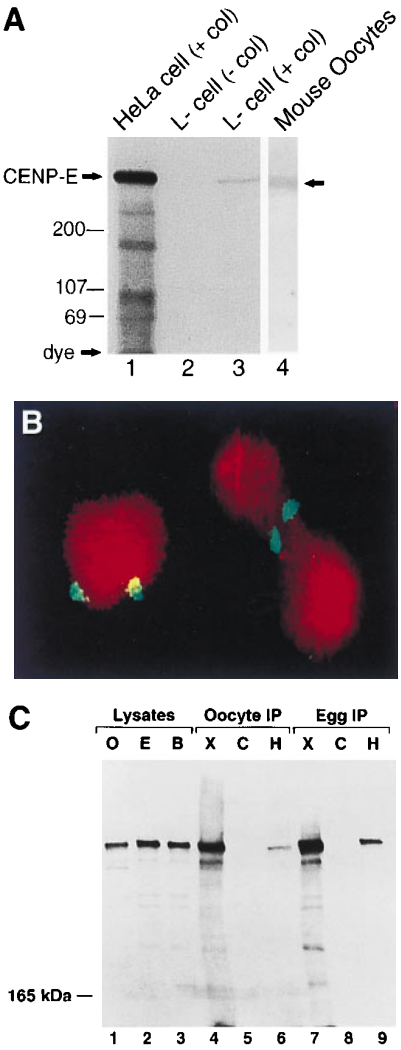

FIG. 1. Immunoblot and immunohistochemical analysis of CENP-E in mitotic cells and ovulated mouse oocytes, and frog oocytes and eggs. (*A*) Total cell lysates prepared from Colcemid-arrested HeLa cells and mouse L-cells, asynchronously growing L-cells, as well as MII-arrested oocytes were subjected to immunoblot analysis with pAb-HpX (1 μg/ml). Lanes: 1, Colcemid-arrested HeLa cells (50 μg total protein); 2, asynchronously growing mouse L cells (100 μg total protein); 3, Colcemid-arrested mouse L cells (100 μg total protein); 4, extract obtained from 1,000 mouse ovulated oocytes. Immunoreactive bands were visualized by autoradiography of ^{125}I-labeled conjugated protein. (*B*) Chromosomes from mitotically arrested L-cells were fixed with cold methanol and immunostained with CENP-E antibody (white) and counter stained with propidium iodide (gray) for visualization of DNA. (*C*) Lysates of oocytes (O; lane 1), eggs (E; lane 2), and 4–8 cell blastulae (B; lane 3) as well as immunoprecipitates of oocytes (lanes 4–6) or eggs (lanes 7–9) performed with pAb-XCEtail (X; lanes 4 and 7), nonspecific rabbit pAb (C; lanes 5 and 8), or pAb-HpX (H; lanes 6 and 9) were separated by electrophoresis upon 4% polyacrylamide gels and subjected to immunoblot analysis with the CENP-E antibody pAb-XCEtail (1:500). Immunoreactive bands were visualized by chemiluminescence of horseradish peroxidase-conjugated secondary antibodies.

whereas CENP-E was not detected in a similar amount of extract from an asynchronous population of cells (Fig. 1*A*, lane 2). Similarly, a whole cell immunoblot of 1,000 mouse eggs revealed an immunoreactive protein with the size expected for CENP-E (Fig. 1*A*, lane 4), and immunocytochemical staining of mitotic chromosomes confirmed that pAb-HpX detected authentic mouse CENP-E at the kinetochores (Fig. 1*B*).

To examine whether CENP-E is a meiotic kinetochore protein, mouse oocytes were selected at 0 h (GV stage), 3 h, 5 h, 7 h (metaphase I; MI), 10 h (just after first polar body extrusion), and 14 h (MII arrested) after initiation of meiotic maturation, and stained for tubulin and CENP-E (pAb-HpX) (Fig. 2). Most of the CENP-E was diffusely localized in the nucleus of GV oocytes (Fig. 2*a*). This localization may be unique to oocytes because in somatic cells CENP-E is located in the cytoplasm (33). As chromosomes condensed during diakinesis, which occurred at ≈3 h after meiotic initiation, CENP-E began to localize to discrete spots on the chromatin (Fig. 2*b*), suggesting that it was associating with kinetochores, as it does in prometaphase of mitosis (31, 33). CENP-E association with kinetochores is maintained during MI of meiosis (Fig. 2 *c* and *d*), and concentrates in the midbody during first polar body extrusion (Fig. 2*e*). Curiously, however, CENP-E could not be detected immunohistochemically in MII-arrested oocytes (Fig. 2*f*), despite the fact that CENP-E protein was detected at the same stage by immunoblot analysis (Fig. 1*A*, lane 4).

CENP-E Is an Essential for Meiotic Progression into Anaphase I. Inhibition of CENP-E function by antibody microinjection has been observed to partially inhibit the transition from metaphase to anaphase in somatic cells (33). However, meiosis I differs greatly from mitosis and meiosis II; during the transition from metaphase to anaphase in meiosis I, homologous chromosomes segregate, whereas in mitosis and meiosis II sister chromatid segregation occurs.

To determine whether CENP-E function is essential for meiotic progression, we injected mouse GV oocytes with pAb-HpX. Greater than 95% (69/72) of oocytes injected with this anti-CENP-E antibody failed to extrude the first polar body and were arrested at MI even after 24 h. By contrast, only 7% (7/99) of uninjected oocytes and 6% (2/35) of control IgG-injected oocytes failed to extrude the first polar body and instead proceeded to MII arrest. Moreover, the injected CENP-E antibodies were observed in a punctate pattern adjacent to the aligned chromosomes (data not shown). Thus, as in mitotic cells, antibody binding to CENP-E efficiently blocks the transition from metaphase to anaphase during meiosis I, strongly supporting the view that CENP-E function is necessary for cell cycle advance past metaphase, both in mitosis and meiosis.

CENP-E Is Modified or Masked During Cell Cycle Arrest at MII. The observation that CENP-E was not detected in MII-arrested oocytes (Fig. 2*f*) suggested that an epitope in the stalk domain of CENP-E was modified or sterically masked, either by structural changes in CENP-E itself or through interaction with other protein(s). To address this possibility, CENP-E staining in MII oocytes was monitored following puromycin activation: puromycin inhibits protein synthesis and induces parthenogenic activation (46). Under these conditions, CENP-E was detected at the midbody during anaphase (Fig. 3*b*) and during second polar body extrusion (Fig. 3*c*) at levels comparable to those observed during meiosis I (Fig. 2). In addition, immunoblotting of mouse eggs revealed that CENP-E was present at MII (Fig. 1*A*, lane 4). These analyses suggest that though the epitope(s) for pAb-HpX is modified or occluded during MII arrest it reappears in the absence of protein synthesis, during the transition to anaphase of meiosis II.

To address whether occlusion of CENP-E is characteristic of MII CSF arrest, we examined the localization of CENP-E

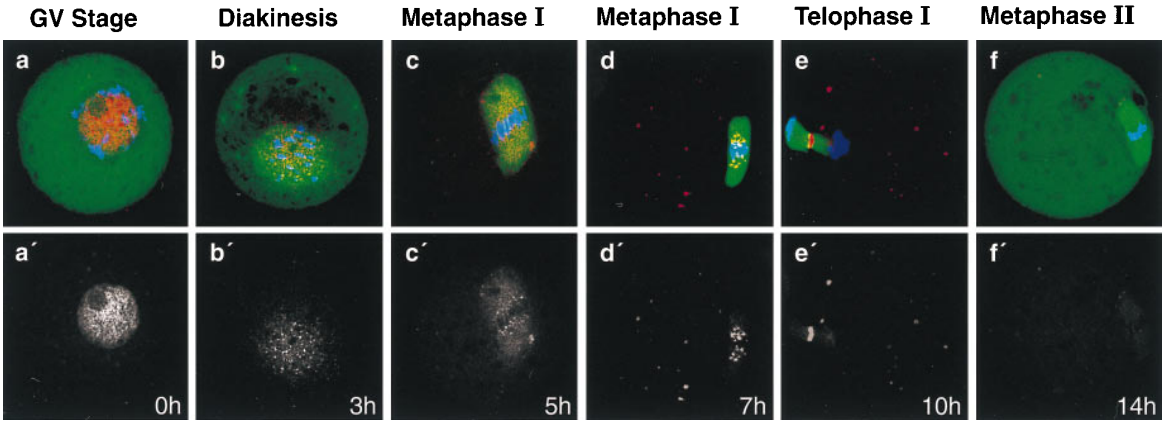

FIG. 2. Stage-specific localization of CENP-E during mouse oocyte maturation. Maturing oocytes at different stages were fixed and stained with anti-CENP-E antibody (pAb-HpX) (red), anti-tubulin antibody (YL1/2) (green), and DAPI (blue) at the indicated time point after meiotic maturation *in vitro*. (*a–f*) Overlay of DAPI, tubulin, and CENP-E staining. (*a′–f′*) Corresponding CENP-E staining only.

during meiosis in *Xenopus* oocytes. To this end, we used pAb-XCEtail, raised against the 556-amino acid C-terminal region of *Xenopus* CENP-E (the full description of *Xenopus* CENP-E will be reported elsewhere). Like pAb-HpX (data not shown), this antibody detected CENP-E (≈340 kDa; data not shown) in lysates of *Xenopus* oocytes, eggs, and 4–8 cell blastulae (Fig. 1*C*, lanes 1–3). pAb-XCEtail also detected CENP-E in *Xenopus* GV lysates, but not in lysates of enucleated oocytes (data not shown), indicating that CENP-E is predominantly a nuclear protein at this stage of meiosis (as previously seen for mouse CENP-E; Fig. 2*a*). To confirm that both antibodies recognized the same protein, each antibody (Fig. 1*C*, lanes 4 and 7 for pAb-XCEtail; lanes 6 and 9 for HpX) as well as control IgG (lanes 5 and 8) was used for immunoprecipitation of oocyte or egg extracts. Immunoblotting of CENP-E with pAb-XCEtail detected a >300-kDa protein in extracts of both oocytes and eggs immunoprecipitated with pAb-HpX or pAb-XCEtail, but not with control IgG. Similar results were obtained if immunoprecipitates were probed with pAb-HpX (data not shown). Thus, pAb-XCEtail and pAb-HpX both recognize authentic frog CENP-E in lysates of *Xenopus* oocytes and eggs.

To determine the localization of CENP-E during *Xenopus* meiosis, cold-treated oocytes were fixed at the time of GV breakdown, when the previously transparent, displaced GV

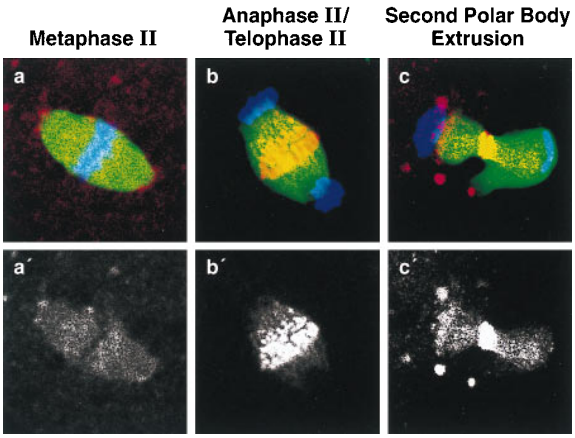

FIG. 3. Detection of CENP-E in parthenogenetically activated mouse oocytes with puromycin. (*a*) Spindles of MII-arrested oocytes prior to activation with puromycin (see *Materials and Methods*). Spindles of oocytes at 2 h (anaphase/telophase) (*b*) and at 4 h (second polar body extrusion) (*c*) after activation were stained with anti-CENP-E antibody pAb-HpX (red), anti-α-tubulin YL1/2 (green), and DAPI (blue). (*a′–c′*, Corresponding CENP-E staining only.)

became opaque, and 3–4 h later at MII. Ovulated eggs were examined prior to, as well as 15 and 30 min after, electric activation at stages corresponding to MII arrest, anaphase II, and telophase II, respectively. pAb-XCEtail detected CENP-E localized to kinetochores at the first meiotic division as well as at MII in both *in vitro* matured oocytes (data not shown) and ovulated eggs (Fig. 4 *a–c*). However, staining became very diffuse or absent at anaphase II (Fig. 4*d*), while 15 min later, at telophase II, CENP-E reappeared at the midbody (Fig. 4*e*). By contrast, pAb-HpX detected CENP-E localized to kinetochores during the first meiotic division (Fig. 4 *f* and *g*), as well as at the spindle poles. However, pAb-HpX did not detect CENP-E at kinetochores in either *in vitro* matured oocytes (data not shown) or ovulated eggs (Fig. 4*h*), despite the observation that pAb-XCEtail could (Fig. 4*c*). These results demonstrate that CENP-E is not diffusely localized at MII but rather that the epitope of CENP-E that is recognized by pAb-HpX is masked at MII. The concordance of these observations with those obtained in mouse oocytes suggests that the mechanism of CENP-E masking during CSF arrest is conserved among vertebrates.

pAb-HpX Epitope of CENP-E Is Not Masked at MII of MOS$^{-/-}$ Oocytes. If the MII masking of CENP-E is related to CSF activity in MII-arrested oocytes, then such modifications should not occur in mice homozygously deleted for Mos which consequently fail to arrest at MII and are spontaneously activated (9–11). To test this, >50 MII-stage MOS$^{-/-}$ oocytes were isolated and stained with pAb-HpX. In all of these oocytes, CENP-E was readily detected at the centromere regions of MII MOS$^{-/-}$ oocytes (Fig. 5 *a* and *a′*) whereas in MOS$^{+/+}$ oocytes it was not (Fig. 5 *b* and *b′*). These results are consistent with the hypothesis that masking of CENP-E plays an important role in MII arrest and that Mos is required for such masking.

DISCUSSION

Microinjection of antibody to CENP-E blocks meiotic progression into anaphase I presumably by disrupting the function of CENP-E and/or adjacent components at meiotic kinetochores. Coupling this with our demonstration that CENP-E is present and kinetochore bound at the earliest meiotic stages and CENP-E's known association with MT motor activity (ref. 32; K.W.W. and D.W.C., unpublished work), indicates that CENP-E is, or associates with, an essential meiotic kinetochore motor in vertebrates.

One key question remaining is why (and how) antibodies to CENP-E block progression to anaphase. Kinetochore components, such as the 3F3 antigen (47, 48) and the transiently

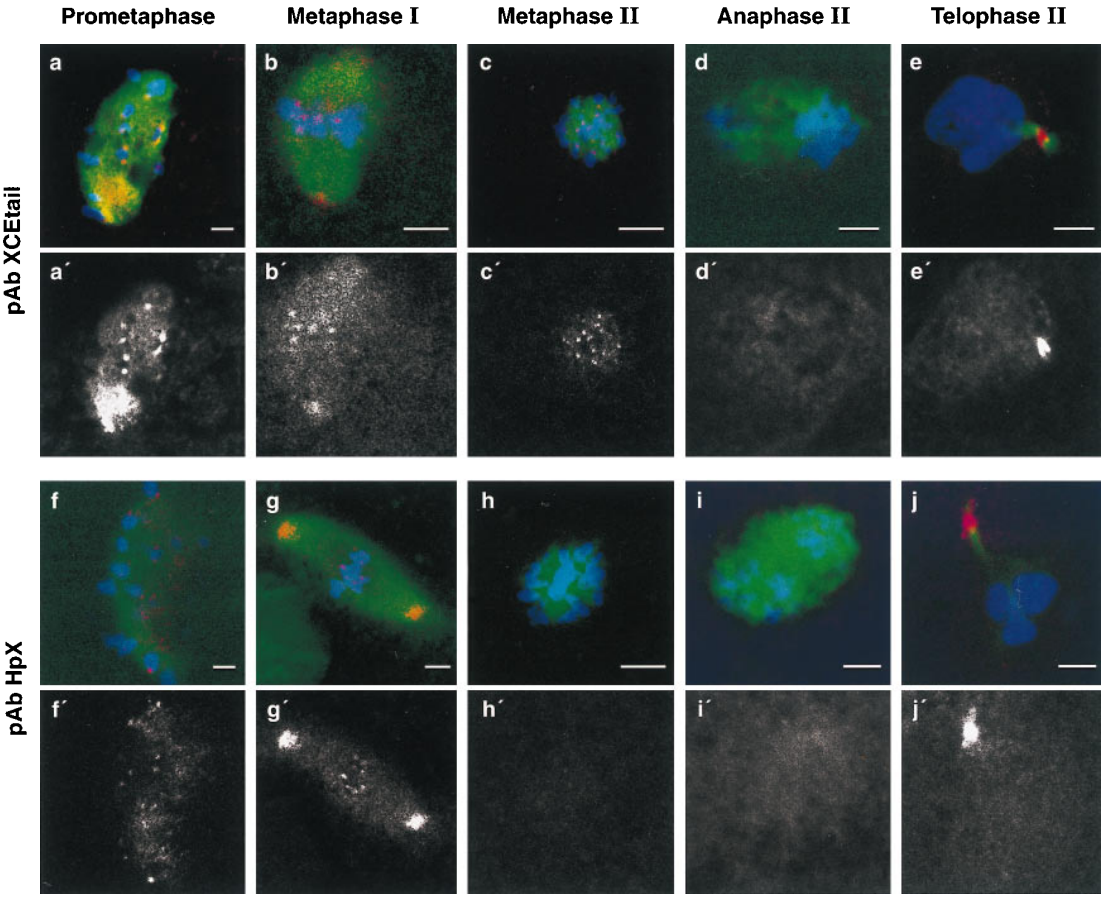

FIG. 4. Detection of CENP-E during frog meiosis. *In vitro* matured prometaphase (*a* and *f*) and MI (*a* and *g*) oocytes as well as MII-arrested eggs (*c* and *h*) and eggs 15 (*d* and *i*) or 30 min after (*e* and *j*) activation were stained with Hoechst 33342 (blue), anti-tubulin (green), and anti CENP-E pAb-XCEtail (*a–e*; red) or pAb-HpX (*f–j*; red). Yellow indicates where CENP-E and tubulin colocalize. (*a′–j′*, Corresponding CENP-E staining only.) All of these confocal images were obtained using the same operating parameters on the confocal laser scanning microscope and subsequently modified in a similar manner to highlight CENP-E staining. The MII images are shown in an axial orientation as the maturing meiotic spindle undergoes an ordered sequence of re-orientations with respect to the animal–vegetal axis. The level of tubulin and Hoechst staining was variable depending upon spindle orientation and the optical plane observed.

associated MAD2 (49, 50), have been linked to a cell cycle "checkpoint" that senses MT attachment to, or alignment of, all chromosomes such that a single unattached kinetochore may produce a transacting signal sufficient to block the transition to anaphase (51, 52). Thus, it is possible that antibody binding to CENP-E may interfere with proper MT attachment (hence, inhibiting CENP-E associated MT motor activity) and/or chromosome alignment, which in turn would activate this kinetochore "checkpoint" signaling pathway.

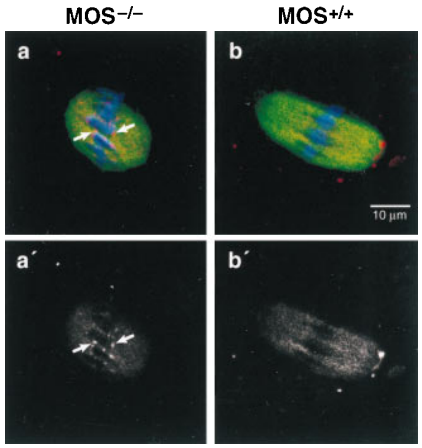

FIG. 5. CENP-E modification identified by pAb-HpX reactivity does not occur at MII in MOS$^{-/-}$ oocytes. GV oocytes were obtained from MOS$^{-/-}$ (*a* and *a′*) or MOS$^{+/+}$ (*b* and *b′*) mice and matured *in vitro*. At 14 h after maturation, oocytes were stained with anti-CENP-E antibody pAb-HpX (red), anti-tubulin antibody (green), and DAPI (blue). (*a* and *b*) Overlay of CENP-E, tubulin, and chromosome staining; (*a′* and *b′*), their corresponding CENP-E staining alone. Arrows indicate CENP-E staining at kinetochores in Mos$^{-/-}$ oocytes.

The hypothesis that CENP-E plays a role in MII arrest is further enhanced by our finding that at least one group of epitopes in the stalk domain of CENP-E is modified or masked in a Mos-dependent manner during the natural arrest arising in MII. Because CENP-E is not similarly masked at MI, the simplest interpretation is that CSF activity results in MII-specific masking of CENP-E, either through modification of CENP-E or binding of kinetochore components that occlude antibody access. Indeed, our observation that CENP-E was readily detected at kinetochores at MII in MOS$^{-/-}$ oocytes (Fig. 5*a*) indicates that the MII-specific masking of CENP-E is a consequence of Mos/MAPK activation and correlates with Mos-induced MII arrest.

It is clear that the masking of CENP-E is at least partially dependent on the Mos/MAPK pathway. However, we do not know whether the masking is caused by modification of CENP-E itself (i.e., phosphorylation) or by association with other proteins specifically expressed (or at least kinetochore-bound) at MII. It is of interest to note that the tail domain of CENP-E has been shown to be specifically phosphorylated by MPF, which prevents the binding of CENP-E to MTs (53).

However, metaphase arrest is not observed in meiosis I even though MPF is activated at similar levels in meiosis I and meiosis II. This indicates that MII-specific factors are required for inhibition of CENP-E activity. Moreover, Mos/MAPK activity alone is not sufficient for the MII-specific masking of CENP-E since the expression of high levels of Mos/MAPK in mos-transformed somatic cells neither arrests the cells at metaphase (20) nor affects the detectability of CENP-E at the kinetochores in those cells (data not shown). Thus, the modification of CENP-E is probably mediated by a protein(s) specifically expressed at MII together with the activation of the Mos protein. The identification of this protein(s) will clarify the molecular mechanisms of CSF-mediated MII arrest.

We thank Peter Donovan, Ira Daar, and Greg Taylor for critically reading the manuscript; Linda Miller and Richard Hudson for technical assistance; Ave Cline and Cheri Rhoderick for preparation of the manuscript; and Richard Frederickson for preparation of the figures. This research was sponsored in part by the National Cancer Institute, Department of Health and Human Services, under contract with ABL, and the G. Harold and Leila Y. Mathers Charitable Foundation and National Institutes of Health Grant GM 29513 (D.W.C.). K.W.W. is the recipient of a Damon Runyon–Walter Winchell postdoctoral fellowship, and K.D.B. was supported by a postdoctoral fellowship from the American Cancer Society.

1. Masui, Y. & Markert, C. L. (1971) *J. Exp. Zool.* **177,** 129–145.
2. Sagata, N., Watanabe, N., Vande Woude, G. F. & Ikawa, Y. (1989) *Nature (London)* **342,** 512–518.
3. Barrett, C. B., Schroetke, R. M., Van der Hoorn, F. A., Nordeen, S. K. & Maller, J. L. (1990) *Mol. Cell. Biol.* **10,** 310–315.
4. Freeman, R. S., Pickham, K. M., Kanki, J. P., Lee, B. A., Pena, S. V. & Donoghue, D. J. (1989) *Proc. Natl. Acad. Sci. USA* **86,** 5805–5809.
5. O'Keefe, S. J., Wolfes, H., Kiessling, A. A. & Cooper, G. M. (1989) *Proc. Natl. Acad. Sci. USA* **86,** 7038–7042.
6. Paules, R. S., Buccione, R., Moschel, R. C., Vande Woude, G. F. & Eppig, J. J. (1989) *Proc. Natl. Acad. Sci. USA* **86,** 5395–5399.
7. Sagata, N., Oskarsson, M., Copeland, T., Brumbaugh, J. & Vande Woude, G. F. (1988) *Nature (London)* **335,** 519–525.
8. Yew, N., Mellini, M. L. & Vande Woude, G. F. (1992) *Nature (London)* **355,** 649–652.
9. Choi, T., Fukasawa, K., Zhou, R., Tessarollo, L., Borror, K., Resau, J. & Vande Woude, G. F. (1996) *Proc. Natl. Acad. Sci. USA* **93,** 7032–7035.
10. Colledge, W. H., Carlton, M. B., Udy, G. B. & Evans, M. J. (1994) *Nature (London)* **370,** 65–68.
11. Hashimoto, N., Watanabe, N., Furuta, Y., Tamemoto, H., Sagata, N., Yokoyama, M., Okazaki, K., Nagayoshi, M., Takeda, N., Ikawa, Y. & Aizawa, S. (1994) *Nature (London)* **370,** 68–71.
12. Mansour, S. J., Matten, W. T., Hermann, A. S., Candia, J. M., Rong, S., Fukasawa, K., Vande Woude, G. F. & Ahn, N. G. (1994) *Science* **265,** 966–970.
13. Nebreda, A. R. & Hunt, T. (1993) *EMBO J.* **12,** 1979–1986.
14. Posada, J., Yew, N., Ahn, N. G., Vande Woude, G. F. & Cooper, J. A. (1993) *Mol. Cell. Biol.* **13,** 2546–2553.
15. Haccard, O., Sarcevic, B., Lewellyn, A., Hartley, R., Roy, L., Izumi, T., Erikson, E. & Maller, J. L. (1993) *Science* **262,** 1262–1265.
16. Minshull, J., Sun, H., Tonks, N. K. & Murray, A. W. (1994) *Cell* **79,** 475–486.
17. Gotoh, Y., Nishida, E., Matsuda, S., Shiina, N., Kosako, H., Shiokawa, K., Akiyama, T., Ohta, K. & Sakai, H. (1991) *Nature (London)* **349,** 251–254.
18. Wang, X. M., Yew, N., Peloquin, J. G., Vande Woude, G. F. & Borisy, G. G. (1994) *Proc. Natl. Acad. Sci. USA* **91,** 8329–8333.
19. Zhou, R., Shen, R., Pinto da Silva, P. & Vande Woude, G. F. (1991) *Cell Growth Differ.* **2,** 257–265.
20. Fukasawa, K. & Vande Woude, G. F. (1995) *Proc. Natl. Acad. Sci. USA* **92,** 3430–3434.
21. Murray, A. & Kirschner, M. (1989) *Nature (London)* **339,** 275–280.
22. Roy, L. M., Singh, B., Gautier, J., Arlinghaus, R. B., Nordeen, S. K. & Maller, J. L. (1990) *Cell* **61,** 825–831.
23. Surana, U., Amon, A., Dowzer, C., McGrew, J., Byers, B. & Nasmyth, K. (1993) *EMBO J.* **12,** 1969–1978.
24. Holloway, S. L., Glotzer, M., King, R. W. & Murray, A. W. (1993) *Cell* **73,** 1393–1402.
25. McKim, K. S., Jang, J. K., Theurkauf, W. E. & Hawley, R. S. (1993) *Nature (London)* **362,** 364–366.
26. Li, X. & Nicklas, R. B. (1995) *Nature (London)* **373,** 630–632.
27. Sawin, K. E. & Endow, S. A. (1993) *BioEssays* **15,** 399–407.
28. Yen, T. J. & Schaar, B. T. (1996) *Cur. Opin. Cell Biol.* **8,** 381–388.
29. Hyman, A. A. & Karsenti, E. (1996) *Cell* **84,** 401–410.
30. Pluta, A. F., Mackay, A. M., Ainsztein, A. M., Goldberg, I. G. & Earnshaw, W. C. (1995) *Science* **270,** 1591–1594.
31. Yen, T. J., Li, G., Schaar, B. T., Szilak, I. & Cleveland, D. W. (1992) *Nature (London)* **359,** 536–539.
32. Thrower, D. A., Jordan, M. A., Schaar, B. T., Yen, T. J. & Wilson, L. (1995) *EMBO J.* **14,** 918–926.
33. Yen, T. J., Compton, D. A., Wise, D., Zinkowski, R. P., Brinkley, B. R., Earnshaw, W. C. & Cleveland, D. W. (1991) *EMBO J.* **10,** 1245–1254.
34. Brown, K. D., Wood, K. W. & Cleveland, D. W. (1996) *J. Cell Sci.* **109,** 961–969.
35. Lombillo, V. A., Nislow, C., Yen, T. J., Gelfand, V. I. & McIntosh, J. R. (1995) *J. Cell Biol.* **128,** 107–115.
36. Choi, T., Aoki, F., Mori, M., Yamashita, M., Nagahama, Y. & Kohmoto, K. (1991) *Development (Cambridge, U.K.)* **113,** 789–795.
37. Duesbery, N. S. & Masui, Y. (1996) *Dev. Genes Evol.* **206,** 110–124.
38. Moses, R. M. & Masui, Y. (1989) *Exp. Cell Res.* **185,** 271–276.
39. Shibuya, E. K., Boulton, T. G., Cobb, M. H. & Ruderman, J. V. (1992) *EMBO J.* **11,** 3963–3975.
40. Choi, T., Rulong, S., Resau, J., Fukasawa, K., Matten, W., Kuriyama, R., Mansour, S., Ahn, N. & Vande Woude, G. F. (1996) *Proc. Natl. Acad. Sci. USA* **93,** 4730–4735.
41. Lohka, M. J. & Maller, J. L. (1985) *J. Cell Biol.* **101,** 518–523.
42. Elinson, R. P. & Rowning, B. (1988) *Dev. Biol.* **128,** 185–197.
43. Gard, D. L. (1992) *Dev. Biol.* **151,** 516–530.
44. Zhang, S. C. & Masui, Y. (1992) *J. Exp. Zool.* **262,** 317–329.
45. Brown, K. D., Coulson, R. M., Yen, T. J. & Cleveland, D. W. (1994) *J. Cell Biol.* **125,** 1303–1312.
46. Siracusa, G., Whittingham, D. G., Molinaro, M. & Vivarelli, E. (1978) *J. Embryol. Exp. Morphol.* **43,** 157–166.
47. Campbell, M. S. & Gorbsky, G. J. (1995) *J. Cell Biol.* **129,** 1195–1204.
48. Gorbsky, G. J. & Ricketts, W. A. (1993) *J. Cell Biol.* **122,** 1311–1321.
49. Hardwick, K. G., Weiss, E., Luca, F. C., Winey, M. & Murray, A. W. (1996) *Science* **273,** 953–956.
50. Li, Y. & Benezra, R. (1996) *Science* **274,** 246–248.
51. Nicklas, R. B., Ward, S. C. & Gorbsky, G. J. (1995) *J. Cell Biol.* **130,** 929–939.
52. Rieder, C. L., Cole, R. W., Khodjakov, A. & Sluder, G. (1995) *J. Cell Biol.* **130,** 941–948.
53. Liao, H., Li, G. & Yen, T. J. (1994) *Science* **265,** 394–398.